IEEE Access
Multidisciplinary | Rapid Review | Open Access Journal

Received February 7, 2017, accepted March 7, 2017, date of publication March 13, 2017, date of current version May 17, 2017.

Digital Object Identifier 10.1109/ACCESS.2017.2681697

Output Predictor-Based Active Disturbance Rejection Control for a Wind Energy Conversion System With PMSG

SHENGQUAN LI[1], (Member, IEEE), AND JUAN LI[1,2]

[1]School of Hydraulic, Energy and Power Engineering, Yangzhou University, Yangzhou 225127, China

[2]Key Laboratory of Measurement and Control of Complex Systems of Engineering, Ministry of Education, Southeast University, Nanjing 210096, China

Corresponding author: Shengquan Li (sqli@yzu.edu.cn)

This work was supported in part by the National Natural Science Foundation of China under Grant 51405428, in part by the Natural Science Foundation of Jiangsu Province under Grant BK20140490, in part by the Open Project Program of Ministry of Education Key Laboratory of Measurement and Control of CSE, under Grant MCCSE2015A01 and Grant MCCSE2016A01, and in part by a Project Funded by the Priority Academic Program Development of Jiangsu Higher Education Institutions.

ABSTRACT Considering the internal and external disturbances in wind energy conversion systems, a predictive active disturbance rejection control (PADRC) strategy for a direct-driven permanent magnet synchronous generator (PMSG)-based wind energy conversion system, is proposed to maximize the wind power extraction in this paper. First, the proposed PADRC method can successfully deal with the effects of the uncertainties in the internal dynamics, modeling error, external forces and the variety of wind speeds, since it inherits the merits of active disturbance rejection control (ADRC). Second, the introduction of Smith Predictor can overcome the time delay in wind turbine system to guarantee the maximum power tracking performance for different wind speeds. Finally, simulation studies are conducted to evaluate power tracking performances of the proposed control strategy. It is shown that the proposed PADRC strategy exhibits significant improvements in both maximum power tracking performance and anti-disturbance ability compared with the traditional ADRC approach.

INDEX TERMS Permanent magnet synchronous generator, wind energy conversion system, active disturbance rejection controller, smith Predictor, maximum power tracking.

I. INTRODUCTION

Global warming and harmful effect of fossil fuel emissions on the climate and environment have boosted worldwide interests in the renewable energy resources [1], [2]. Among them, wind energy as a new pollution-free and inexhaustible resource is extensively developed in recent decades due to the probable depletion, high costs, and negative environmental impacts of conventional energy sources. Among currently available wind energy conversion systems (WECSs), there are mainly two kinds of operation mode of generator, i.e., the fixed speed mode, and the variable speed mode. The variable speed wind turbines are preferable to fixed speed ones, since the variable speed wind turbines have simpler structure with more stability, lower mechanical stress, smaller aerodynamic noise. Moreover, the variable speed wind turbines can capture the maximum power over a wide range of wind speed by adjusting the generator's speed to be its optimal one. The direct-driven PMSG has been widely applied in WECSs owing to its competitive advantages, such as gearless construction, high power density, little noise, high efficiency, good reliability, easy maintenance [3]. In addition, the direct-driven PMSG can possibly be operated at low speeds but still achieve high torques. It is well-known that the main control purpose for the wind turbine in the low speed region is the power efficiency maximization. Thus, in order to achieve optimum wind energy extraction from the wind turbine below the rated wind speed, the wind turbine generator should be operated in variable-speed mode. To achieve this goal, the tip speed ratio should be maintained at its optimum value despite variation of wind speed. Due to stochastic characteristics of natural wind, along with the aerodynamic characteristics of a wind turbine, the WECS are essential non-linear systems [4], [5]. In addition, the performance of WECS is interrupted by lumped disturbances, including internal disturbances, i.e., parameter variations, control couplings, modeling errors and nonlinear dynamics of the plant, and external disturbances which mainly come from wind gusting, torsional vibration, wind stream dissymmetry, etc [6], [7]. The lumped

disturbances cause the parameter variations, large power fluctuations and unavoidable vibrations with detrimental effects to wind turbines. So the anti- disturbance ability of wind turbine is a significant task to capture the optimal power in real time.

Over the past few decades, numerous feedback control strategies have been exploited to improve the efficiency and power quality of wind turbine equipped with PMSG [8]–[11]. Although these conventional feedback based maximum power point tracking methods can finally suppress them through feedback regulation in a relatively slow way, they usually cannot react directly and fast enough to reject the lumped disturbances. Moreover, wind turbines are expected to work effectively under wide range of wind speeds. Therefore, the control designs for wind energy conversion systems become more significant. Since the sliding mode control (SMC) shows a good robustness for anti - disturbances, it is widely used in WECS. To deal with the problem of controlling power generation in variable speed wind turbines, a high-order sliding-mode control strategy is proposed to maximize the generated power from wind turbine in [12]. The proposed strategy presents excellent dynamic performance robust against parametric uncertainties and lumped disturbances. Commonly, the SMC faces an unavoidable application problem which is known as chattering. This can degrade the tracking performance when the WECS encounters severe disturbances. Hence, we should rationally design the control algorithm for maximum power tracking of the WECS, with the aim of obtaining robustness of the whole closed-loop system. Unfortunately, the accurate model of WECS is difficult to obtain and lumped disturbances cannot be directly measured or require costly sensors, which bring many challenges to control algorithm design.

The active disturbance rejection controller (ADRC) is a novel robust control method to attenuate internal and external disturbances. A nonlinear ADRC method is originally proposed by Han in 1995 [13], and then fully articulated in 2009 after more than ten years' developments [14]. Compared with the model-based control methods, the ADRC can be designed without the detailed mathematical model. The essence of ADRC is that both the internal uncertainties and external disturbances, i.e., lumped disturbances, can be estimated by an extended state observer (ESO), then the effect of lumped disturbances can also be compensated by the feed-forward channel with the estimated value. On the basis of nonlinear ADRC proposed by Han, a structure of linear ADRC (LADRC) with the advantages of nonlinear ADRC, is proposed by Gao for the practical industrial applications [15]. The LADRC simplifies the controller design and reduces the difficulty in tuning, analysis and implementation. Due to these promising features, the LADRC, as a new control design framework, has become increasingly popular and been widely investigated in recent years. Nowadays, the LADRC has been widely applied to various industrial areas, such as motor system [16], robotic system [17], maglev system [18], structural vibration [19], energy conversion systems [20], tower cranes [21], and non-minimum phase system [22]. However, the employment of ADRC into PMSG-based wind energy conversion system is rather new.

Compared with the conventional strategies in WECSs, the LADRC has some advantages, such as little requirement of information about the plant dynamics, simple structure, excellent ability of disturbance rejection. But LADRC also has some limitations for WECS, especially in certain situations with high inertia, strong nonlinearity, rapid parameters perturbations, and large random external disturbances. Under such circumstances, ESOs may not estimate lumped disturbance accurately. In order to solve the problem of severe lumped disturbances in PMSG based WECS, the authors proposed a model-based ADRC method with the available model information into an ESO to efficiently compensate the lumped disturbances [2].

Besides theses severe disturbances, the time delay is also a major issue of control system design for the excellent performance of WECSs with LADRC method. The time delay of WECS may arise from many terms, including computational delay, the finite response time of the inner current loop and sensor, the mechanical coupling, and the transmission characteristics [23]. The time delay will give rise to current waveforms distortion, voltage losses and torque pulsation torque pulsation. Thus, the time delay in WECS also poses a serious challenge. Considering the characteristics of WECS, this paper aims to deal with the critical issue in WECS based on direct-driven (PMSG): the attenuation of the effects of disturbances and the time delay, with the aim of extracting maximum power from the wind turbine below the rated speed. In this paper, ADRC is a proposed control solution to the PMSG-based WECS. Since the Smith Predictor is a specifically method to solve the problem of time delay in control systems, a novel predictive ADRC (PADRC) based on Smith Predictor is introduced to the variable speed wind turbines to deal with the challenges of lumped disturbances and the time delay in WECS.

The rest of this paper is organized as follows. The dynamics of PMSG based wind turbine are described in **Section II**. The control scheme of the proposed PADRC for PMSG is illustrated in **Section III**. Simulation researches with several kinds of wind types are carried out to verify the superiority of the proposed PADRC method in **Section IV**. The conclusions are given in the last.

II. WIND TURBINE SYSTEM DESCRIPTION

A. WIND TURBINE MODELING

The mechanical power P_m extracted by a variable speed wind turbine from the natural wind is expressed as follows [24]:

$$P_m = \frac{1}{2}\rho\pi R^2 C_P(\lambda, \beta)v^3, \tag{1}$$

The mechanical torque of the wind turbine can be described as,

$$T_m = 0.5\rho\pi C_P(\lambda, \beta)R^3 v^2/\lambda, \tag{2}$$

where ρ, R, v and λ are the air density, the blade radius, wind speed and tip-speed ratio, respectively. The parameter C_p denotes the power coefficient of wind turbine, which depends on the blades' aerodynamic design and operating conditions. It is a nonlinear function of the blade pitch angle β and the tip-speed ratio λ, which is given by (3), as indicated in [24]:

$$\lambda = \frac{\omega R}{v}, \tag{3}$$

where ω is the angular velocity of rotor (rad/s). The parameter $C_p(\lambda, \beta)$ can be expressed by the following equation [24],

$$C_p(\lambda, \beta) = 0.22\left(\frac{116}{\lambda_i} - 0.4\beta - 5\right)e^{-\frac{12.5}{\lambda_i}} + 0.0068\lambda, \tag{4}$$

where $\frac{1}{\lambda_i} = \frac{1}{\lambda+0.08\beta} - \frac{0.035}{\beta^3+1}$.

The typical curves of C_p versus λ is obtained in [2]. According to Eq. (1), for a given value of wind speed v, the maximum power exaction is achieved when C_p takes its maximum value. Therefore, the power coefficient C_p for each β can reach a maximum value at the optimum tip-speed ratio λ_{opt}. The maximum power coefficient $C_{pmax}(C_p = 0.48)$ can been achieved when $\beta = 0$ and $\lambda = 8$. And from Eq.(3), it can be obtained that the output power is the maximum at the optimum speed ω_{opt} for a certain v, which corresponds to the optimum tip speed ratio λ_{opt}. Therefore, the wind turbine should be always operated at λ_{opt} to extract maximum power at variable wind speed when the wind speeds are below the rated speed of wind turbine. The speed of wind turbine should be equal to the optimum speed ω_{opt} to achieve the optimum power extraction.

B. PMSG MODELING

According to the theory of the space vector, the stator voltage equations for PMSG can be represented in the rotating d-q reference frame as follows [24], [25],

$$\begin{cases} u_d = L_d\dfrac{di_d}{dt} + R_s i_d - L_q n\omega i_q \\ u_q = L_q\dfrac{di_q}{dt} + R_s i_q + L_d n\omega i_d + n\omega\psi_f \end{cases} \tag{5}$$

where u_d, u_q and i_d, i_q are the stator voltages and currents in the direct and quadrature axis of rotor, respectively. The parameters R_s, ψ_f and n are the resistance of stator windings, the magnet flux and the pair of poles, respectively. The parameters L_d, L_q are the d-q inductances of the stator windings, here $L_q = L_d = L$. The electromagnetic torque T_e of PMSG can be given as Eq.(6):

$$T_e = \frac{3}{2}n\psi_f i_q. \tag{6}$$

The rotor dynamics of wind turbine can be described as follows:

$$J\frac{d\omega}{dt} = T_m - B_v\omega - T_e, \tag{7}$$

where J (kg $\cdot$ m^2) represents the total inertia, B_v (kg $\cdot$ m^2/s) is the viscous friction coefficient, and T_m (N $\cdot$ m) denotes the drive torque.

III. CONTROL DESIGN

A. ADRC BASED ON SMITH PREDICTOR

Note that the ESO can deal with the uncertainties of the system. In order to achieve superior performance, the ADRC concept is introduced to design the controller for lumped disturbances. With the dynamic compensation of the estimation information, the speed loot for system (7) is reduced to a double integrator. Consider the following system dynamics.

$$J\dot{\omega} = F + g(\omega, t) + w \tag{8}$$

where F is the control variable, w is the external disturbances, t is the time and $g(\omega, t)$ is a time-varying function of angular velocity. So the original system (8) is reformulated as,

$$\dot{\omega} = b_0 u + f(\omega, w, t) \tag{9}$$

where b_0 is the parameter related to system model, $f(\omega, w, t)$ is the lumped disturbances, which includes not only the external disturbances but also the unknown internal dynamics. Then the state vector of the systems can be defined as $\boldsymbol{x} = \begin{bmatrix} x_1 & x_2 \end{bmatrix}^T = \begin{bmatrix} \omega & f \end{bmatrix}^T$, which has two components. Note that for a first-order system the stat vector is normally defined as $x = [\omega]$ with one state variable. The variable $x_2 = f$, representing the lumped disturbances, is an extended state variable of the first-order system.

The state space representation of Eq. (9) is defined as:

$$\begin{cases} \dot{\boldsymbol{x}} = \boldsymbol{A}\boldsymbol{x} + b_0\boldsymbol{B}\boldsymbol{u} + \boldsymbol{E}\dot{f} \\ y = \boldsymbol{C}\boldsymbol{x} \end{cases} \tag{10}$$

where $\boldsymbol{A} = \begin{bmatrix} 0 & 1 \\ 0 & 0 \end{bmatrix}$, $\boldsymbol{B} = \begin{bmatrix} 1 \\ 0 \end{bmatrix}$, $\boldsymbol{E} = \begin{bmatrix} 0 \\ 1 \end{bmatrix}$, and $\boldsymbol{C} = \begin{bmatrix} 1 & 0 \end{bmatrix}$.

An extended state space form of Eq. (10) is designed as:

$$\dot{\hat{\boldsymbol{x}}} = \boldsymbol{A}\hat{\boldsymbol{x}} + b\boldsymbol{B}\boldsymbol{u} + \boldsymbol{L}(x_1 - \hat{x}_1) \tag{11}$$

where $\hat{\boldsymbol{x}} = \begin{bmatrix} \hat{x}_1 & \hat{x}_2 \end{bmatrix}^T$ are the observer vector of the state vector $\boldsymbol{x}$, and b represents the estimation of b_0. The vector $\boldsymbol{L} = \begin{bmatrix} l_1 & l_2 \end{bmatrix}^T$ is the observer gain vector. Therefore, the ADRC of Eq.(11) can be expressed as follows for this SISO system.

$$u = k_1(y^* - \hat{x}_1) - \hat{x}_2/b \tag{12}$$

where y^* and k_1 are the expected output value and controller gain of feedback channel, respectively. Combining the above Eq.(10), the state variable $\hat{x}_1$ is an estimate of the output y.

Unfortunately, the ADRC controller with the structure (12) cannot directly handle the system time delay. It is well-known that Smith Predictor is an effective strategy to deal with the effect of time delays. The idea of incorporating the Smith Predictor technique, as shown in Fig. 1, is to have the controller act on the system without the delayed part. The tracking performance of the input wind speeds is significantly improved, since the proposed ADRC based on Smith Predictor method can provide a faster reaction to the changes in the system. According to the substance of the Smith Predictor method and the characteristics of the system, in order to solve the problems of lumped disturbances and time delay,

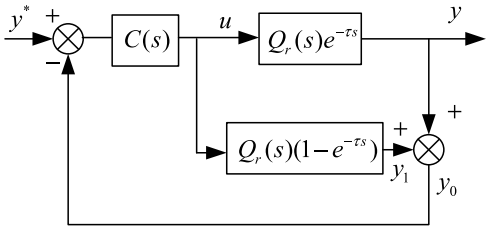

FIGURE 1. Classical structure of smith predictor.

simultaneously, the transfer function of whole system can be shown as Eq. (13),

$$Q(s) = Q_r(s)e^{-\tau s}, \tag{13}$$

where $Q(s)$ and $Q_r(s)$ describe the transfer function form of plant with time delay and the normal model, respectively. The parameter τ is the time delay coefficient.

From Fig. 1, we can obtain that $y = Q_r(s)e^{-\tau s}u$ and $y_1 = Q_r(s)(1 - e^{-\tau s})u$, respectively. Thus, it can be seen that the auxiliary output variable y_0 is introduced to offset the effect of the delay loop, which is represents as:

$$y_0 = y + y_1 = Q_r(s)e^{-\tau s}u + Q_r(s)(1 - e^{-\tau s})u = Q_r(s)u \tag{14}$$

According to Eq. (14), the transfers function between u and y_0 does not contain time delay loop. When time delay τ is a small constant, Eq. (14) can be further rewritten as:

$$\begin{aligned} y_0 &= Q_r(s)u = Q_r(s)e^{-\tau s}(\frac{1}{e^{-\tau s}})u \\ &= e^{\tau s}Q_r(s)e^{-\tau s}u \approx (1+\tau s)y = y + \tau s y = y + \tau\dot{y} \end{aligned} \tag{15}$$

The last term of Eq. (15) indicates that the auxiliary output y_0 can be obtained from the system output y and its differential $\dot{y}$. So the significant part in the controller design is to get an effective differentiation of y with the property of strong against noise.

In conventional PID implementation, the differentiation of output y is obtained approximately as:

$$\frac{s}{\tau s + 1}y = \frac{1}{\tau}(1 - \frac{1}{\tau s + 1})y \tag{16}$$

Eq.(16) can also be rewritten in the following time domain,

$$\dot{y}(t) \approx \frac{1}{\tau}(y(t) - y(t - \tau)) \tag{17}$$

It indicates that if $y(t)$ contains noise $n(t)$, from Eq. (17). The noise $n(t)$ will be amplified by the factor of $1/\tau$ in $\dot{y}(t)$. Therefore, this kind of approximation is quite sensitive to the noise. To solve this problem, the following approximation equation is employed in this paper.

$$\dot{y}(t) \approx \frac{y(t - t_1) - y(t - t_2)}{t_2 - t_1}, \quad t_2 > t_1 > 0, \tag{18}$$

And the delay signal $y(t - t_1)$ can be obtained via first-order inertial part $1/(t_1 s + 1)$. So the transfer function of the approximate differential equation can be described as follows,

$$g_d(s) = \frac{s}{t_1 t_2 s^2 + (t_1 + t_2)s + 1}. \tag{19}$$

Thus, the control law of PADRC can be constructed in following Eq. (20),

$$\begin{cases} \dot{z}_1 = z_2 - 2p(z_1 - y_0) + b_0 u \\ \dot{z}_2 = -p^2(z_1 - y_0) \\ y_0 = y + \tau\dot{y} \end{cases} \tag{20}$$

where z_1 is the estimate of auxiliary output y_0, z_2 is the estimate of lumped disturbances of the system, b_0 is an estimate of b, and p is the observer bandwidth of ESO. Generally, the larger the observer bandwidth p is, the more accurate the estimation will be. However, a large observer bandwidth will increase noise sensitivity. Therefore, an appropriate observer bandwidth should be selected as a compromise between the tracking performance and the noise tolerance.

It can be seen from Eq. (20) that the auxiliary variable y_0 can be obtained from the actual output of the system y and its derivative $\dot{y}$. So the proposed PADRC based on the Smith Predictor method can be described as the following remark.

Remark: First, the auxiliary variable y_0 can be estimated through the ESO strategy using the actual output of the system y and its derivative $\dot{y}$ based on Eq. (17). Then, the new form of the PADRC strategy can be designed based on the auxiliary output variable y_0 to solve the time delay of wind turbine system. Thus, the novel control law of the ADRC method for wind energy conversion system can be given as Eq. (21),

$$u = k_p(y^* - z_1) - z_2/b_0 \tag{21}$$

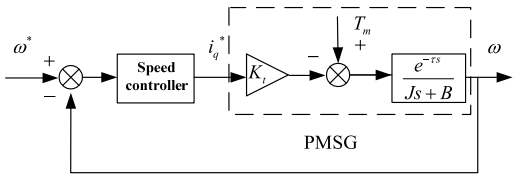

FIGURE 2. Structure of speed control for PMSG with time delay.

B. THE PROPOSED PADRC DESIGN FOR PMSG

A system configuration of a vector-controlled PMSG drive with time delay is shown in Fig. 2. where $K_t = (3/2)n\psi_f$. The time delay coefficient τ may arise from computational delay, the finite response time of the inner current loop and sensor, and other significant delay depends on the mechanical coupling and the transmission characteristics. The parameter ω^* is the desired speed output from the wind turbine blade.

According to Eq. (7), the speed output of PMSG can be obtained as follows,

$$\dot{\omega} = \frac{T_m}{J} - \frac{B}{J}\omega + b_0 i_q = f + b_0 i_q \tag{22}$$

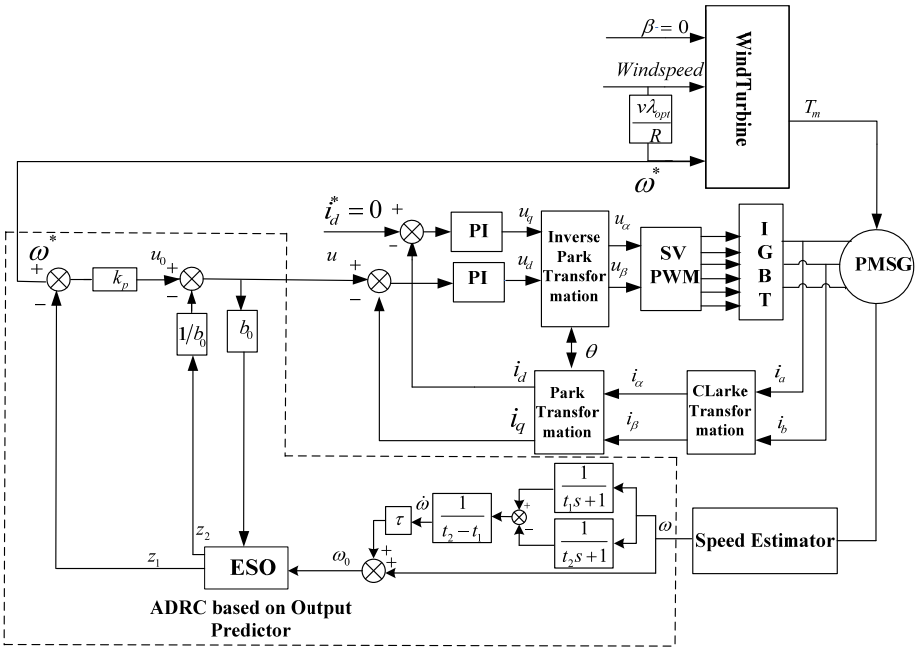

FIGURE 3. The scheme of the proposed PADRC for wind turbine based on PMSG.

TABLE 1. Specification of the PMSG based wind turbine.

PMSG parameters		Wind Turbine parameters	
Rotor inertial (kg·m2)	2×10^{-3}	Air density(kg/m3)	1.25
Permanent magnetic flux (Wb)	0.175	Optimum tip speed ratio	8
Stator inductance L(H)	8.5×10^{-3}	Basic wind speed(m/s)	6
Pole pairs	4	Turbine blade radius(m)	1.5
Stator resistance(Ω)	2.875	Maximum power coefficient	0.48
Viscous coefficient(N·ms/rad)	8.29×10^{-5}	Ttime delay(ms)	30
Rated Power (kW)	7.5	Rated wind speed (m/s)	37.5
Rated voltage (V)	380	Rated speed (rpm)	1500

where $b_0 = -K_t/J$. The function $f = (T_m/J) - (B/J)\omega$ represents the lumped disturbances, including the friction, the unknown internal dynamics, the external disturbances, the tracking error of the current loop i_q, and the modeling error. Assuming that f is globally differentiable, the speed control loop of PMSG is reduced to a first-order system.

Then, the augmented state space form of the dynamic system can be obtained as follows,

$$\begin{cases} \dot{x}_1 = x_2 + bi_q \\ \dot{x}_2 = h \end{cases} \tag{23}$$

where the parameter $h = df/dt = \dot{f}$ represents the differential of lumped disturbances. And the corresponding ESO of the speed control system for PMSG is designed as follows,

$$\begin{cases} \dot{z}_1 = z_2 - l_1(z_1 - \omega_0) + b_0 u \\ \dot{z}_2 = -l_2(z_1 - \omega_0) \end{cases} \tag{24}$$

where z_1 is the estimation of speed output. The parameter z_2 is the estimation of unknown lumped disturbance f_i. And $\omega_0 = \omega + \tau\dot{\omega}$ is the auxiliary speed output. The parameters l_1 and l_2 are the observer gains for different state variables. The observer gains are chosen such that the characteristic polynomial $s^2 + l_1 s + l_2$ is Hurwitz. Similar as [19], the ESO of the speed control loop can be chosen as,

$$\begin{cases} \dot{z}_1 = z_2 - 2p(z_1 - \omega_o) + b_0 u \\ \dot{z}_2 = -p^2(z_1 - \omega_o) \\ \omega_o = \omega + \tau\dot{\omega} \\ u = k_p(\omega_o^* - z_1) - z_2/b_0 \end{cases} \tag{25}$$

The observer bandwidth p should be well designed, so the outputs of ESO z_1 and z_2 can track ω_o and f, respectively. By ignoring the effect of f using z_2, the scheme of the proposed PADRC for PMSG is shown in Fig.3.

IV. RESULTS AND ANALYSIS

To demonstrate the tracking performance of proposed PADRC strategy, comparative simulation studies with traditional ADRC are carried out in this section.

The parameters of PMSG-based WECS without connecting to the grid are shown in Table 1. A nomenclature summarizing all the symbols throughout this brief is furnished

TABLE 2. Nomenclature.

Symbol	Description [unit]	Symbol	Description [unit]
$\boldsymbol{A}$	System Matrix of Eq.(10)	T_m	Mechanical torque of the wind turbine[N·m]
$\boldsymbol{B}$	Input Matrix of Eq.(10)	u	Control variable
B_v	viscous friction coefficient[kg•m^2/s]	u_d , u_q	Stator voltage in the *d*-*q* axis[V]
$\boldsymbol{C}$	Output Matrix of Eq.(10)	V_b	Base wind speed [m/s]
C_p	Power coefficient of wind turbine	V_g	Gust wind speed [m/s]
F	Turbulence scale	V_n	Noise wind speed [m/s]
K_N	Surface drag coefficient	V_N	natural wind speed [m/s]
i_d , i_q	Stator current in the *d*-*q* axis[A]	V_r	Ramp wind speed [m/s]
J	total inertia [kg•m^2]	v	Wind speed [m/s]
$\boldsymbol{L}$	Observer gain vector	$\hat{\boldsymbol{x}}$	Observer vector of $\boldsymbol{x}$
L_d , L_q	*d*-*q* inductances of the state windings [H]	$\boldsymbol{x}$	The state vector
n	Pair of poles	y^*	Expected output
p	Observer bandwidth of ESO	y_0	Auxiliary output in Eq.(20)
P_m	Mechanical power from wind [W]	y	Actual output
$Q(s)$	Transfer function with time delay	$\boldsymbol{z}$	Observer vector of PMSG
$Q_r(s)$	Transfer function of the normal model	ψ_f	Magnet flux [Wb]
R	Blade radius [m]	λ	Tip-speed ratio
R_s	Resistance of stator windings [Ω]	ρ	Air density [kg/m^3]
S_v	Spectral density function	ω	Angular velocity of rotor [rad/s]
T_e	electromagnetic torque [N·m]	β	Blade pitch angle[°]

in Table 2. For fair comparisons, firstly, the control inputs of the two algorithms have the same saturation limit; secondly, each algorithm achieves good tracking performance by carefully tuning the parameters of controller. According to the principle of separation, it is very easy to obtain the parameters of feedback part (k_p) and the observer bandwidth of the ESO (p) via the Try and Error method. The parameters are $K_p = 30$, $b = 209$, $p = 96$ for traditional ADRC and are $K_p = 10, b = 209, p = 300$ for the proposed PADRC, respectively. The two control methods can both achieve excellent tracking performances.

A. THE WIND SPEED MODEL

As is discussed above, wind is the significant factor to the performance of WECS. The variations of wind speeds have the great influence on the system performance of power generator. Thus, relevant wind model, corresponding to the real wind, should be established to discuss the dynamic performance of WECS. Similar to [2], [26], [27], the wind is constructed by the linear combination of base wind, ramp wind, gust wind and noise wind in this paper. So, the wind model is defined as following Eq. (26),

$$V_N = V_b + V_g + V_r + V_n, \tag{26}$$

where V_b is the base wind speed, V_g is the gust wind speed, V_r is the ramp wind speed, V_n is the noise wind speed. And the profile of the wind speed is given in Fig.4.

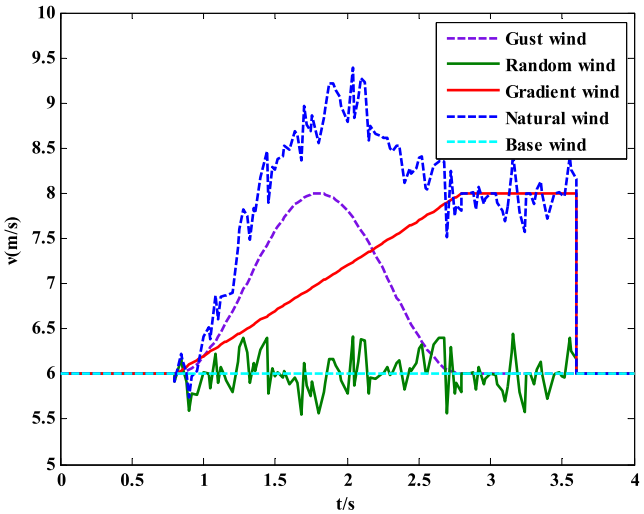

FIGURE 4. The profiles of different winds.

B. SIMULATION RESULTS AND ANALYSIS

1) CASE 1: THE BASE WIND SIMULATION

The base wind always exists in the wind energy conversion systems. Generally, the speed of base wind without change over time, can be regarded as a constant. The base wind speed is usually used to study the power of grid available from PMSG, due to the fact that it reflects the changes of mean wind speed in wind farm. The base wind-speed

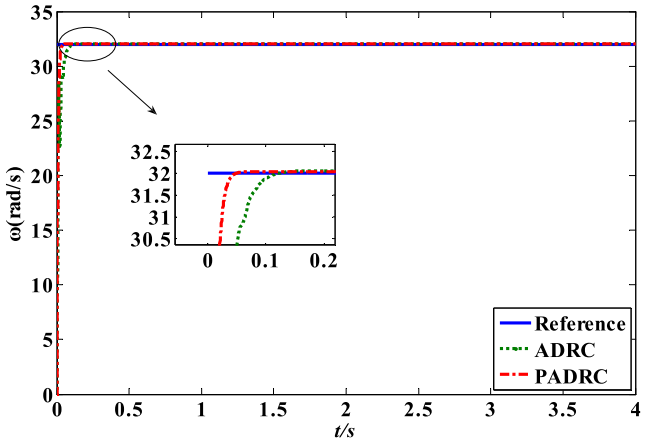

FIGURE 5. The base wind speed tracking.

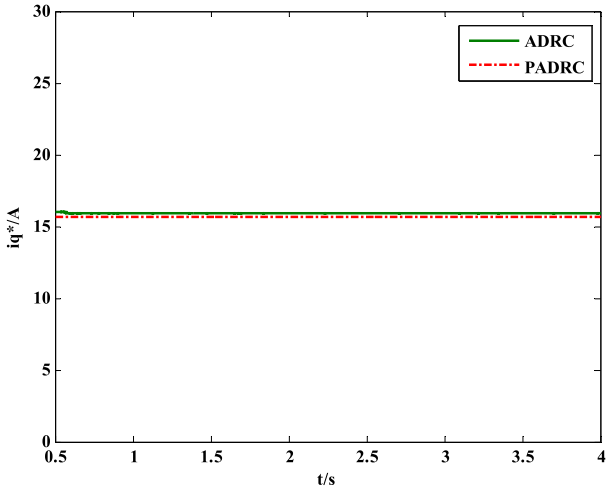

FIGURE 6. The control effects of different ADRC strategies for the base wind.

component can be expressed by the following Eq. (27).

$$V_b = K_b, \tag{27}$$

where K_b is a constant , and the base wind speed is 6m/s.

The simulation results of speed tracking performance and the control effects of different ADRC strategies for the base wind are shown in Figs. 5 and 6.

2) CASE 2: THE GUST WIND SIMULATION

In order to describe the characteristic of a sudden change in wind speed, the gust wind is introduced to model the wind speed. The gust is widely used in the research of WECS, since it can provide a theoretical basis for the study of the dynamic analysis of wind energy conversion system, and the impact of PMSG on the grid voltage fluctuation. The gust specific mathematical relationship can be described as follows,

$$V_g = \begin{cases} 0, & t < t_{1g} \\ v_{\cos}, & t_{1g} < t < t_{1g} + T_g \\ 0, & t < t_{1g} + T_g, \end{cases} \tag{28}$$

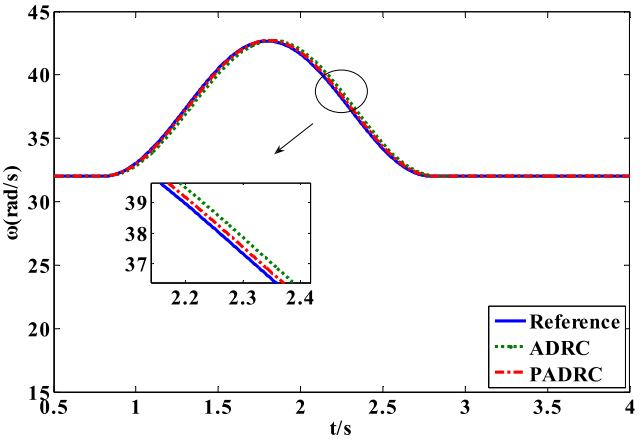

FIGURE 7. The gust wind speed tracking.

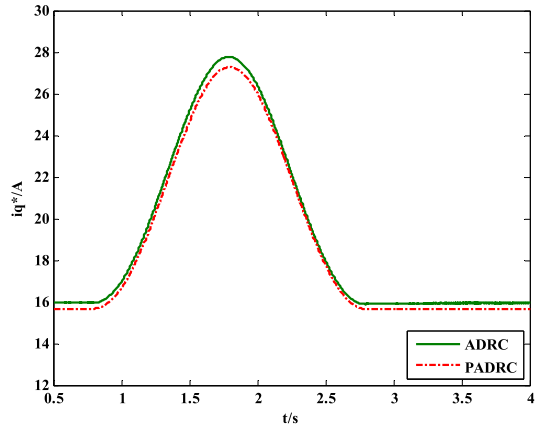

FIGURE 8. The control effects of different ADRC strategies for the gust wind.

where $v_{\cos} = \frac{G_{\max}}{2}[1-\cos 2\pi((t/T_g)-(t_{1g}/T_g))]$, and V_g, $v_{\cos}$ represent the gust speed. The parameter t_{1g} is the gust starting time, T_g is the gust period, and $G_{\max}$ is the maximum value of the gust. In this case study, the gust begins at 0.8s, terminates at 2.8s, where the period is 2s, and the gust's maximum speed is 8m/s. The comparison curves of the speed tracking performances and controller outputs for the gust wind are shown in Figs. 7 and 8.

3) CASE 3: THE RAMP WIND SIMULATION

To describe the characteristics of a slow change in wind speed, a ramp wind is employed for the model of wind speed. In this paper, the ramp wind can be described as follows.

$$V_r = \begin{cases} 0, & t < t_{1r} \\ v_{ramp}, & t_{1r} < t < t_{2r} \\ 0, & t > t_{2r}, \end{cases} \tag{29}$$

where $v_{ramp} = R_{\max}(1 - \frac{t-t_{2r}}{t_{1r}-t_{2r}})$, and V_r, v_{ramp} represent the wind speed at different times. The parameters t_{1r}, t_{2r} are the starting time and terminal time respectively. The parameter $R_{\max}$ is the maximum of ramp wind. In this example, the ramp begins at 0.8s, and terminates at 3.6s. The maximum speed of ramp is 8m/s. The comparison simulation results of the speed

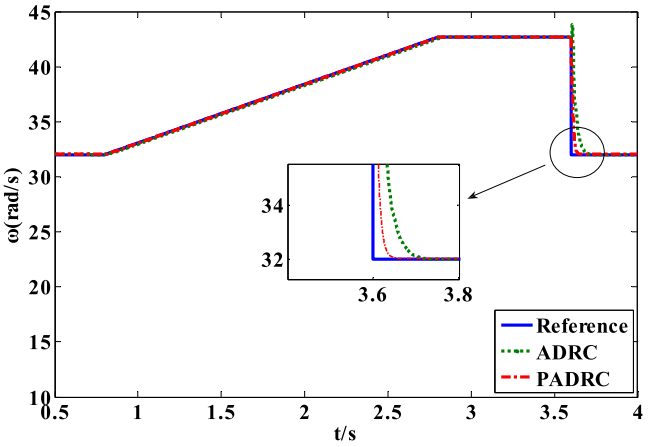

FIGURE 9. The ramp wind speed tracking.

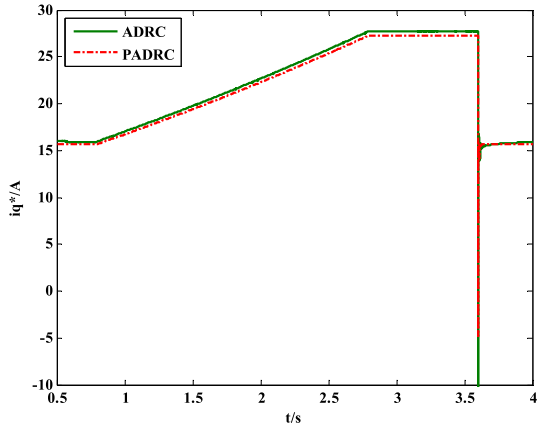

FIGURE 10. The control effects of different ADRC strategies for the ramp wind.

tracking performance and the controller output for the ramp wind are shown in Figs. 9 and 10.

4) CASE 4: THE RANDOM (STOCHASTIC) WIND SIMULATION

This kind of winds are featured with stochastic random in the relative height. The random wind is introduced in this case. The random wind speed component can be expressed by the following Eq. (30) in this paper.

$$V_N = 2\sum_{i=1}^{N}\sqrt{S_V(\omega_i)\Delta\omega}\cos(\omega_i + \varphi_i), \tag{30}$$

where $\omega_i = (1 - 1/2)\Delta\omega$ is a random variable with uniform probability density on the interval $(0, 2\pi)$ and $\Delta\omega = (0.5 - 2.0)$ rad/s. The parameter φ_i is also a random variable with uniform probability density on the interval $(0 \sim 2\pi)$, and the spectral density function $S_V(\omega_i)$ with respect of ω_i can be defined as the following Eq. (31),

$$S_V(\omega_i) = \frac{2K_N F^2 |\omega_i|}{\pi^2\left[1 + (F\omega_i/\bar{v}\pi)^2\right]^{4/3}}, \tag{31}$$

where K_N is the surface drag coefficient, F is the turbulence scale, and $\bar{v}$ is the mean wind speed. In this paper, it is assumed $N = 50$, $F = 2000$, $K_N = 0.004$.

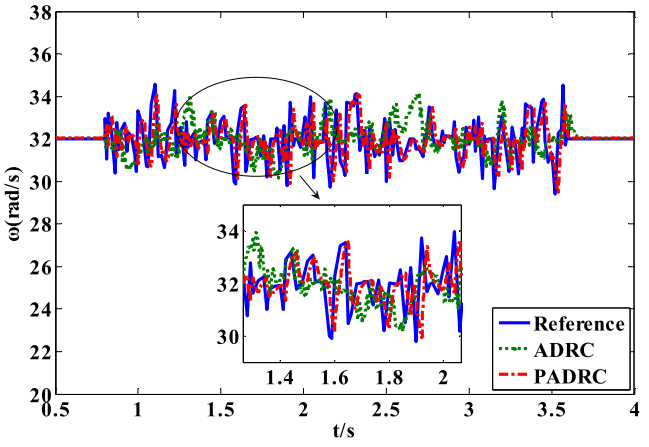

FIGURE 11. The random wind speed tracking.

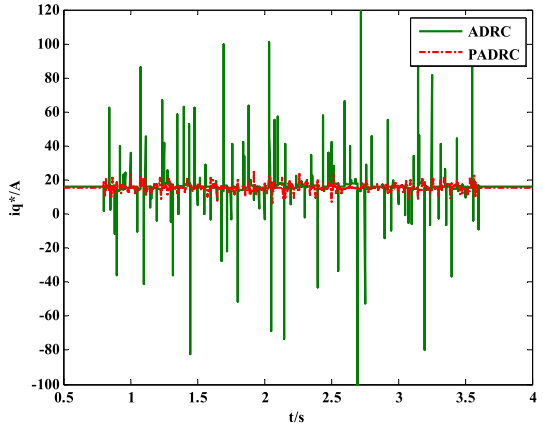

FIGURE 12. The control effects of different ADRC strategies for the random wind.

Figs. 11 and 12 describe the simulation results of the speed tracking performance and the controller output response comparison curves in the random wind. The random wind begins at 0.8s, and terminates at 3.6s in this case.

5) CASE 5: THE NATURAL WIND SIMULATION

It is well known that the natural wind is the main energy source of wind turbine, and is featured with strong mutation and randomness. Since the natural wind consists of the above four kinds of wind, it can be defined by the following Eq. (32),

$$V_N = V_b + V_g + V_{ramp} + V_n \tag{32}$$

Figs. 13 and 14 show the simulation results of speed tracking performance and control output response comparison curves in the natural wind.

The integral of absolute error (IAE) performance index is employed here to estimate the control performance of tracking performance with five wind types. Values of the performance index in five cases are list in Table 3. Since the sampling frequency is 1kHz in this control system, there are 4000 data samples for each case. It can be observed that the IAE of the five wind types under the proposed PADRC scheme are much smaller than that under the traditional ADRC scheme.

TABLE 3. The integral of absolute error (IAE) index for different control methods with five wind types.

	Base wind		Gust wind		Ramp wind		Random wind		Natural wind	
	ADRC	PADRC	ADRC	PADRC	ADRC	PADRC	ADRC	PADRC	ADRC	PADRC
IAE	102.1	89.2	150.3	100.7	273	162.3	620.5	261.9	828.3	323.7

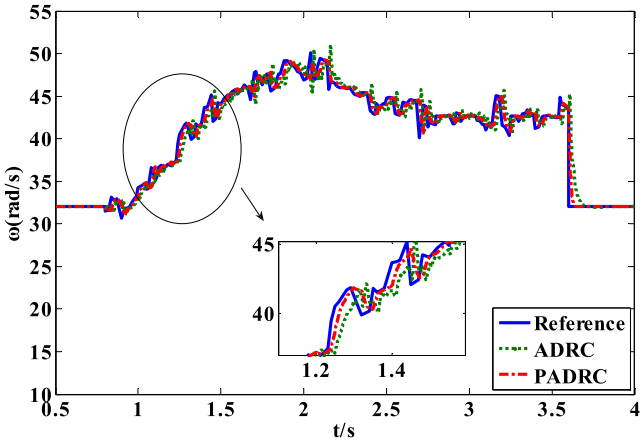

FIGURE 13. The natural wind speed tracking.

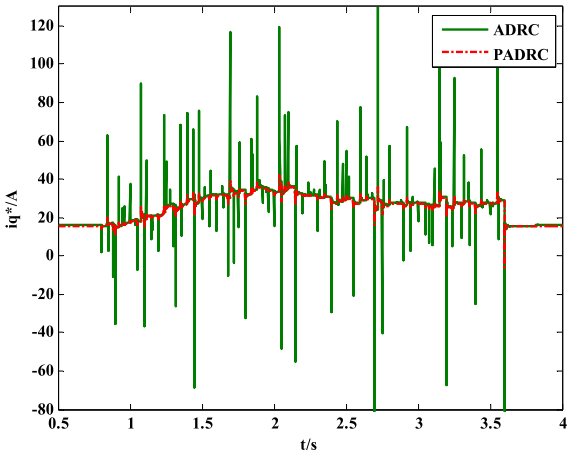

FIGURE 14. The control effects of different ADRC strategies for the natural wind.

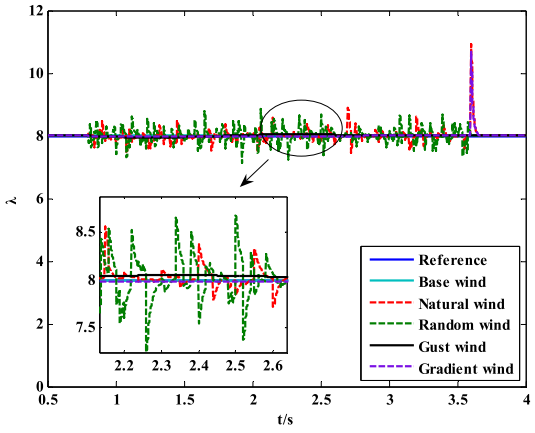

FIGURE 15. The tip-speed ratio.

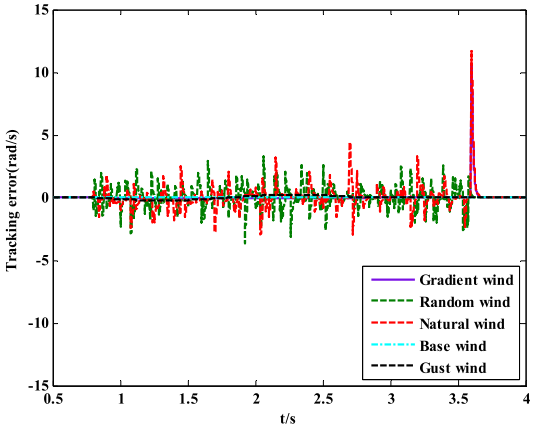

FIGURE 16. The tracking error in different wind types.

It can be observed from Figs. 5, 7 and 9 that the simulation results of wind speed show very similar tracking performances between the traditional ADRC and PADRC, when the wind speed keeps constant or changes in a small scale. And from Figs. 6, 8 and 10, we can see that the control signals are nearly the same in steady-state. Since the output rotor speed and the system disturbances change relatively little in the first three cases, the time delay has little effect on the system tracking performance. And the ESO itself can estimate the disturbances and compensate them through the feedback channel.

However, as shown in Figs.11 and 13, the output rotor speed of PADRC system tracks the reference trajectory better than that of the traditional ADRC system, when the wind changes rapidly. And from Figs. 12 and 14, we can see that the absolute values of control signals of PADRC system are much smaller than that of the traditional ADRC system in steady-state. In this paper, the tracking error and the tip-speed ratio of PADRC system are plotted in Figs. 15 and 16, respectively. As shown in Figs.15 and 16, the tip-speed ratio remains near the optimum value $\lambda_{opt} = 8$, and the tracking error is near zero, which shows good tracking performance. The system disturbances increase sharply with wind speed changing in a large scale. The ESO itself can't deal with the rapid disturbances and the effect from time delay thoroughly with the traditional ADRC, due to the existence of time delay and the disturbances. In contrast, the PADRC can well compensate the time delay and deal with disturbances, since it introduces the Smith Predictor to eliminating the effect of time delay. So the proposed PADRC show a better speed tracking performance and smaller control variable in such situations. According to these simulation results, it can be concluded that the PADRC possesses a better dynamic performance than the traditional ADRC strategy.

V. CONCLUSION

A direct-driven PMSG variable speed WECS, as a nonlinear uncertain dynamic system, is analyzed in this paper. The ADRC strategy, which can deal with uncertainties and large scale variations under different operating conditions, is introduced to realize the maximum output power of the generator for different kinds of wind. The time delay existing in the WECS, caused by computational delay, the finite response time of the inner current loop and sensor, mechanical coupling and the transmission characteristics, can significantly degrade the maximum power point tracking performance of the WECS. To this end, a PADRC based on the Smith Predictor is further proposed to improve the control performance. Finally, the proposed PADRC is successfully validated by simulation studies. Simulation results demonstrate that the proposed control strategy can effectively deal with time delays and exhibit strong robustness against lumped disturbances.

REFERENCES

[1] X. S. Hu, S. J. Moura, N. Murgovski, B. Egardt, and D. P. Cao, "Integrated optimization of battery sizing, charging, and power management in plug-in hybrid electric vehicles," *IEEE Trans. Control Syst. Technol.*, vol. 24, no. 3, pp. 1036–1043, Mar. 2016.
[2] S. Q. Li, K. Z. Zhang, J. Li, and C. Liu, "On the rejection of internal and external disturbances in a wind energy conversion system with direct-driven PMSG," *ISA Trans.*, vol. 61, pp. 95–103, Mar. 2016.
[3] J. W. Chen, J. Chen, and C. Y. Gong, "On optimizing the aerodynamic load acting on the turbine shaft of PMSG-based direct-drive wind energy conversion system," *IEEE Trans. Ind. Electron.*, vol. 61, no. 8, pp. 4022–4033, Aug. 2009.
[4] D. Q. Dang, Y. Wang, and W. Cai, "Offset-free predictive control for variable speed wind turbines," *IEEE Trans. Sustain. Energy*, vol. 4, no. 1, pp. 2–10, Jan. 2013.
[5] C. Zhe, J. M. Guerrero, and F. Blaabjerg, "A review of the state of the art of power electronics for wind turbines," *IEEE Trans. Power Electron.*, vol. 24, no. 8, pp. 1859–1875, Aug. 2009.
[6] S. D. Glidden, "Wind turbine with drive train disturbance isolation," U.S. Patent 4 329 117 A, May 11, 1982.
[7] A. Uehara *et al.*, "A coordinated control method to smooth wind power fluctuations of a PMSG-based WECS," *IEEE Trans. Energy Convers.*, vol. 26, no. 2, pp. 550–558, Feb. 2011.
[8] C. L. Xia, X. Gu, and T. N. Shi, "Neutral-point potential balancing of three-level inverters in direct-driven wind energy conversion system," *IEEE Trans. Energy Convers.*, vol. 26, no. 1, pp. 18–29, Jan. 2011.
[9] A. Harrag and S. Messalti, "Variable step size modified P&O MPPT algorithm using GA-based hybrid offline/online PID controller," *Renew. Sustain. Energy Rev.*, vol. 49, pp. 1247–1260, Sep. 2015.
[10] A. E. Magri, F. Giri, G. Besançon, A. E. Fadili, L. Dugard, and F. Z. Chaoui, "Sensor less adaptive output feedback control of wind energy systems with PMS generators," *Control Eng. Pract.*, vol. 21, no. 4, pp. 530–543, 2012.
[11] Y. Zhu, M. Cheng, W. Hua, and W. Wang, "A novel maximum power point tracking control for permanent magnet direct drive wind energy conversion systems," *Energies*, vol. 5, no. 5, pp. 1398–1412, 2012.
[12] B. Beltran, T. Ahmed-Ali, and M. Benbouzid, "High-order sliding-mode control of variable-speed wind turbines," *IEEE Trans. Ind. Electron.*, vol. 56, no. 9, pp. 3314–3321, Sep. 2009.
[13] J. Q. Han, "A class of extended state observers for uncertain systems," *Control Decision*, vol. 10, no. 1, pp. 85–88, 1995.
[14] J. Q. Han, "From PID to active disturbance rejection control," *IEEE Trans. Ind. Electron.*, vol. 56, no. 3, pp. 900–906, Mar. 2009.
[15] Z. Q. Gao, "Scaling and bandwidth parameterization based controller tuning," in *Proc. Amer. Control Conf.*, Denver, CT, USA, 2003, pp. 4989–4996.
[16] H. Sira-Ramírez, J. Linares-Flores, C. García-Rodríguez, and M. A. Contreras-Ordaz, "On the control of the permanent magnet synchronous motor: An active disturbance rejection control approach," *IEEE Trans. Control Syst. Technol.*, vol. 22, no. 5, pp. 2056–2063, Sep. 2014.
[17] L. A. Castaneda, A. Luviano-Juarez, and I. Chairez, "Robust trajectory tracking of a delta robot through adaptive active disturbance rejection control," *IEEE Trans. Control Syst. Technol.*, vol. 23, no. 4, pp. 1387–1398, Jul. 2015.
[18] S. H. Li, J. Yang, and W. H. Chen, "Generalized extended state observer based control for systems with mismatched uncertainties," *IEEE Trans. Ind. Electron.*, vol. 59, no. 6, pp. 4792–4802, Dec. 2012.
[19] S. Q. Li, J. Li, and Y. P. Mo, "Piezoelectric multimode vibration control for stiffened plate using adrc-based acceleration compensation," *IEEE Trans. Ind. Electron.*, vol. 61, no. 12, pp. 6892–6902, Dec. 2014.
[20] X. Li, Y. Sun, M. Su, and H. Wang, "Coordinated control for unbalanced operation of stand-alone doubly fed induction generator," *Wind Energy*, vol. 17, no. 2, pp. 317–336, 2014.
[21] N. Sun, Y. C. Fang, H. Chen, B. Lu, and Y. M. Fu, "Slew/translation positioning and swing suppression for 4-DOF tower cranes with parametric uncertainties: Design and hardware experimentation," *IEEE Trans. Ind. Electron.*, vol. 63, no. 10, pp. 6407–6418, Oct. 2016.
[22] L. Sun, D. H. Li, and Z. Q. Gao, "Combined feedforward and model-assisted active disturbance rejection control for non-minimum phase system," *ISA Trans.*, vol. 64, pp. 24–33, Sep. 2016.
[23] Y. A.-R. I. Mohamed, "Adaptive self-tuning speed control for permanent-magnet synchronous motor drive with dead time," *IEEE Trans. Energy Convers.*, vol. 21, no. 4, pp. 855–862, Apr. 2006.
[24] J. Zaragoza, J. Pou, A. Arias, C. Spiteri, E. Robles, and S. Ceballos, "Study and experimental verification of control tuning strategies in a variable speed wind energy conversion system," *Renew. Energy*, vol. 36, no. 5, pp. 1421–1430, 2011.
[25] H. Shariatpanah, R. Fadaeinedjad, and M. Rashidinejad, "A new model for PMSG-based wind turbine with yaw control," *IEEE Trans. Energy Convers.*, vol. 28, no. 4, pp. 929–937, Apr. 2013.
[26] Y. L. Wei, S. X. Han, and S. Z. Shi, "The modeling and simulation of the combined wind speed in the wind power system," *Renew. Energy*, vol. 28, no. 2, pp. 18–20, 2010.
[27] R. N. Dao, K. Q. L. Meng, and Q. Zhang, "Improvement and modeling simulation of combined wind speed in the wind power system by Rayleigh probability distribution," *Renew. Energy*, vol. 32, no. 4, pp. 461–465, 2014.

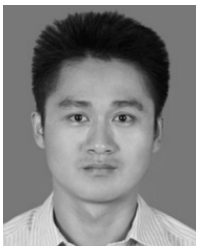

SHENGQUAN LI (M'15) was born in Changde, China, in 1982. He received the B.S degree from the Department of Automatic Control, Hunan University of Arts and Science, Changde, in 2005, and the M.S degree from the School of Automation, Anhui University of Technology, Maanshan, China, in 2008, and the Ph.D. degree in mechatronics from the School of Aerospace Engineering, Nanjing University of Aeronautics and Astronautics, Nanjing , China, in 2012.

He is currently an Associate Professor with the School of Hydraulic, Energy and Power Engineering, Yangzhou University. His research interests include disturbance estimation and compensation and its application to WECSs.

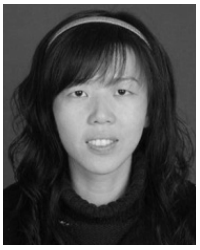

JUAN LI was born in Linyi, China, in 1983. She received the B.S. degree from the Department of Automatic Control, Weifang Medical University, Wei Fang, China, in 2006, the M.S. degree from the School of Automation, Anhui University of Technology, Maanshan, China, in 2009, and the Ph.D. degree from the School of Automation, Southeast University, Nanjing, China, in 2013.

She is currently a Lecture with the School of Hydraulic, Energy and Power Engineering, Yangzhou University. Her main research interest is active anti-disturbance control.